

Production of the new gauge boson B_H via $e^- \gamma$ collision in the littlest Higgs model*

WANG Xue-Lei(王学雷)¹⁾ JIN Zhen-Lan(金振兰) ZENG Qing-Guo(曾庆国)

(College of Physics and Information Engineering, Henan Normal University, Xinxiang 453007, China)

Abstract The lightest new gauge boson B_H with mass of hundreds GeV is predicted in the littlest Higgs model. B_H should be accessible in the planned ILC and the observation of such particle can strongly support the littlest Higgs model. The realization of $\gamma\gamma$ and $e^- \gamma$ collisions would open a wider window to probe B_H . In this paper, we study the new gauge boson B_H production processes $e^- \gamma \rightarrow e^- \gamma B_H$ and $e^- \gamma \rightarrow e^- Z B_H$ at the ILC. Our results show that the production cross section of the process $e^- \gamma \rightarrow e^- Z B_H$ is less than 0.1 fb in most parameter spaces allowed by the electroweak precision data while the cross section of the process $e^- \gamma \rightarrow e^- \gamma B_H$ can be over one fb in the favorable parameter spaces. With the high luminosity, the enough typical signals could be produced via $e^- \gamma \rightarrow e^- \gamma B_H$. Because the final electron and photon beams can be easily identified and the signal can be easily distinguished from the backgrounds produced by Z and H decaying, $e^- \gamma \rightarrow e^- \gamma B_H$ is a promising process to probe B_H .

Key words the littlest Higgs model, cross section, new gauge boson B_H , the decay modes of B_H

PACS 12.60.Cn, 14.80.Cp, 13.66.Hk

1 Introduction

The Standard Model (SM) of particle physics is a remarkably successful theory. It provides a complete description of physics at currently accessible energies, and its predictions have been confirmed to high accuracy by the high energy experiments. However, the mechanism of electroweak symmetry breaking (EWSB) remains unknown. Furthermore, in the SM, the Higgs mass receives quadratically divergent quantum corrections which have to be cancelled by some new physics (NP) to avoid fine-tuning. The SM Higgs sector is therefore an effective theory below some cut-off scale Λ . To avoid fine-tuning of Higgs mass, one would require the NP scale Λ to be \sim TeV. Various NP models have been proposed at the TeV scale, which can cancel the quadratic divergences of the Higgs mass. Recently, a new theory, dubbed the little Higgs theory^[1], has drawn a lot of interests as a new candidate to solve the problems mentioned above.

So far, a number of specific little Higgs models^[2–5] have been proposed. The generic structure of these

models is that a global symmetry is broken at the scale f which is around a TeV. At the scale f , there are new gauge bosons, scalars, fermions responsible for canceling the one loop quadratic divergences to the Higgs mass from the SM particles. The new particles predicted by the little Higgs models may produce the characteristic signatures at the present or future high energy collider experiments^[6]. Among the various little Higgs models, the most economical and phenomenologically viable model is the littlest Higgs model^[5] which realizes the little Higgs idea and has all essential features of the little Higgs models. Such model consists of a nonlinear σ model with a global $SU(5)$ symmetry which is broken down to $SO(5)$ by a vacuum expectation value (vev) of order $f \sim \Lambda_s/4\pi \sim$ TeV. At the same time, the gauge subgroup $[SU(2) \times U(1)]^2$ is broken to its diagonal subgroup $SU(2)_L \times U(1)_Y$, identified as the SM electroweak gauge group. This breaking scenario gives rise to four massive gauge bosons (B_H, Z_H, W_H^\pm). Thus, study of the possible signatures of the new gauge bosons and their contributions to some processes at high-energy colliders is a good method to

Received 23 April 2007, Revised 17 July 2007

* Supported by National Natural Science Foundation of China (10375017, 10575029)

1) E-mail: wangxuelei@sina.com

test the littlest Higgs model and furthermore to probe the EWSB mechanism. In the littlest Higgs model, the masses of these new heavy gauge bosons are in the range of a few TeV, except for the mass of B_H in the range of hundreds GeV. The gauge boson B_H is the lightest new particle in the littlest Higgs model so that it should be the first signal at future experiments and would play the most important role in testing the littlest Higgs model.

It is well known that the LHC can directly probe the possible NP beyond the SM up to a few TeV. If new particles or interactions can be directly discovered at the future hadron collider experiments, the linear e^+e^- collider(LC) will then play a crucial role in the detailed study of these new phenomena and in the reconstruction of the underlying fundamental theories. In addition to e^+e^- physics, the future LC provides a unique opportunity to study $\gamma\gamma$ and $e\gamma$ interactions at high energy and luminosity comparable to those in e^+e^- collisions^[7]. High energy photon beams for $\gamma\gamma$, $e\gamma$ collisions(Photon Collider) can be obtained by Compton backscattering of laser light off the high energy electrons. Such possibilities will be realized at the International Linear Collider(ILC), with the center of mass (c.m.) energies $\sqrt{s} = 300 \text{ GeV} - 1.5 \text{ TeV}$ and the yearly luminosity 500 fb^{-1} ^[8]. The physics programs at the Photon Collider are very rich which can complement the physics programs of the e^+e^- mode. The Photon Collider will considerably contribute to the detailed understanding of new phenomena, and in some scenarios it is the best instrument for the discovery of NP elements. In particular, the $e^-\gamma$ collision can produce the particles which are not kinematically accessible via e^+e^- collision at the same collider^[7, 9]. Moreover, the high energy photon polarization can vary relatively easily, which is advantageous for experiments. All the virtues of the Photon Collider provide good chances to pursue NP particles, specially the lightest new gauge boson B_H which should be kinematically accessible at the planned ILC. Some B_H production processes have been studied at the Photon Collider^[10, 11]. In Ref. [10], we have studied the process of the B_H production associated with W boson pair via $\gamma\gamma$ collision, i.e., $\gamma\gamma \rightarrow W^+W^-B_H$. Such process would offer a good chance to probe the B_H signal and to study the triple and quartic gauge couplings involving B_H and the SM gauge bosons which shed important light on the symmetry breaking features of the littlest Higgs model. Via $e\gamma$ collision, B_H can also be produced at the TeV energy LC. An important B_H production process via $e\gamma$ collision is $e^-\gamma \rightarrow e^-B_H$ which has been studied in Ref. [11], and the study shows that the B_H should be detectable via

such process. We find that there exist other interesting B_H production processes via $e\gamma$ collision, i.e., $e^-\gamma \rightarrow e^-\gamma B_H$ and $e^-\gamma \rightarrow e^-ZB_H$. In this paper, we study the possibility of detecting B_H via these processes and complement the probe of the new gauge boson B_H via $e\gamma$ collision.

This paper is organized as follows. In Sec. 2, we briefly review the littlest Higgs model. Sec. 3 presents the calculations of the production cross sections of the processes. The numerical results and conclusions are shown in Sec. 4.

2 The littlest Higgs model

In this section, we describe the main ideas of the littlest Higgs model^[5] and the detailed review of this model can be found in Ref. [6]. Furthermore, the phenomenologies of this model have also been discussed in great detail in precision tests and low energy measurements^[12–15].

The littlest Higgs model embeds the electroweak sector of the SM in a $SU(5)/SO(5)$ non-linear sigma model. The breaking of the global $SU(5)$ symmetry to a $SO(5)$ subgroup at the scale $\Lambda_s \sim 4\pi f$ by a vev of order f , results in 14 Goldstone bosons, which are denoted by $\Pi^a(x)$. We can conveniently parameterize the Goldstone bosons by the non-linear sigma model field

$$\Sigma(x) = e^{i\Pi/f} \Sigma_0 e^{i\Pi^T/f} = e^{2i\Pi/f} \Sigma_0, \quad (1)$$

where f is the decay constant, and $\Pi(x) = \sum_{a=1}^{14} \Pi^a(x) X^a$. The sum runs over the 14 broken $SU(5)$ generators X^a and here we have used the relation $X^a \Sigma_0 = \Sigma_0 X^{aT}$, obeyed by the broken generators, in the last step.

The leading order dimension-two term in the non-linear sigma model can be written for the scalar sector as

$$\mathcal{L}_\Sigma = \frac{f^2}{8} \text{Tr}\{(D_\mu \Sigma)(D^\mu \Sigma)^\dagger\}, \quad (2)$$

and the covariant derivative is

$$D_\mu \Sigma = \partial_\mu \Sigma - i \sum_{j=1}^2 [g_j (W_{\mu j} \Sigma + \Sigma W_{\mu j}^T) + g'_j (B_{\mu j} \Sigma + \Sigma B_{\mu j}^T)]. \quad (3)$$

$W_{\mu j}$, $B_{\mu j}$ are the $SU(2)_j$ and $U(1)_j$ gauge fields, respectively and g_j , g'_j are the corresponding coupling constants.

Furthermore, the vev breaks the gauge subgroup $[SU(2) \times U(1)]^2$ of $SU(5)$ down to the diagonal group $SU(2)_L \times U(1)_Y$, identified as the SM electroweak group. So four of the fourteen Goldstone bosons are

eaten to give masses to four particular linear combinations of the gauge fields

$$\begin{aligned} W &= sW_1 + cW_2, & W' &= -cW_1 + sW_2, \\ B &= s'B_1 + c'B_2, & B' &= -c'B_1 + s'B_2, \end{aligned} \quad (4)$$

with the mixing angle

$$\begin{aligned} s &\equiv \sin \psi = \frac{g_2}{\sqrt{g_1^2 + g_2^2}}, & c &\equiv \cos \psi = \frac{g_1}{\sqrt{g_1^2 + g_2^2}}, \\ s' &\equiv \sin \psi' = \frac{g_2'}{\sqrt{g_1'^2 + g_2'^2}}, & c' &\equiv \cos \psi' = \frac{g_1'}{\sqrt{g_1'^2 + g_2'^2}}. \end{aligned} \quad (5)$$

These couplings can be related to the SM couplings (g, g') by

$$\frac{1}{g^2} = \frac{1}{g_1^2} + \frac{1}{g_2^2}, \quad \frac{1}{g'^2} = \frac{1}{g_1'^2} + \frac{1}{g_2'^2}. \quad (6)$$

At the scale f , the SM gauge bosons W and B remain massless while the heavy gauge bosons acquire masses of order f

$$m_{W'} = \frac{g}{2sc}f, \quad m_{B'} = \frac{g'}{2\sqrt{5}s'c'}f. \quad (7)$$

The presence of $\sqrt{5}$ in the denominator of $m_{B'}$ leads to a relatively light new neutral gauge boson.

The Higgs boson at tree level remains massless as a Goldstone boson, but its mass is radiatively generated because the nonlinearly realized symmetry is broken by the gauge, Yukawa, and self-interactions of the Higgs field. The little Higgs models introduce a collective symmetry breaking: Only when multiple gauge symmetries are broken is the Higgs mass radiatively generated; the loop corrections to the Higgs boson mass occur at least at the two-loop level. The one-loop quadratic divergences induced by the SM particles are canceled by those induced by the new particles due to the exactly opposite couplings. For example, at leading order in $1/f$, the couplings of Higgs field to the gauge bosons following from Eq. (2) are given as

$$\begin{aligned} \mathcal{L} &= \frac{1}{4}H(g_1g_2W_1^{\mu a}W_{2\mu}^a + g_1'g_2'B_1^{\mu}B_{2\mu})H^+ + \dots = \\ &\frac{1}{4}H[g^2(W_\mu^a W^{\mu a} - W_\mu'^a W'^{\mu a}) - \\ &g'^2(B_\mu B^\mu - B'_\mu B'^\mu)]H^+ + \dots \end{aligned} \quad (8)$$

It is to be compared with SUSY models where the cancellation occurs due to the different spin statistics between the SM particle and its superpartner.

In order to cancel the severe quadratic divergence from the top quark loop, a pair of colored Weyl Fermions \tilde{t}, \tilde{t}^c , with the SM quantum numbers $(3, 1)_{Y_1}$ and $(\bar{3}, 1)_{-Y_1}$, are also required in addition to the usual third-family weak doublet $q_3 = (t_3, b_3)$ and weak singlet u_3^c . Vector like field $\chi = (b_3, t_3, \tilde{t})$ will replace the third-family SM quark doublet and u_3^c, \tilde{t}^c

are the corresponding right handed singlets. The couplings of the SM top quark to the pseudo-Goldstone bosons and the heavy vector pair in the littlest Higgs model are given as

$$\begin{aligned} \mathcal{L} &= \frac{1}{2}\lambda_1 f \epsilon_{ijk} \epsilon_{xy} \chi_i \Sigma_{jx} \Sigma_{ky} u_3^c + \lambda_2 f \tilde{t} \tilde{t}^c + \text{h.c.} = \\ &-i\lambda_1 (\sqrt{2}h^0 t_3 + i f \tilde{t} - \frac{i}{f} h^0 h^{0*} \tilde{t}) u_3^c + \text{h.c.} + \dots \end{aligned} \quad (9)$$

ϵ_{ijk} and ϵ_{xy} are the antisymmetric tensors. As it is shown in the above equation, the quadratic divergence from the top quark is canceled by that from the new heavy top-quark-like fermion. In addition, the cancellation is stable against radiative corrections.

The EWSB is induced by the remaining Goldstone bosons H and ϕ . Through radiative corrections, the gauge, the Yukawa, and self-interactions of the Higgs field generate a Higgs potential which triggers the EWSB. Now the SM W, Z bosons acquire masses of order v , and small (of order v^2/f^2) mixing between the heavy gauge bosons and the SM gauge bosons W, Z occurs. The masses of the SM gauge bosons W, Z and their couplings to the SM particles are modified from those in the SM at the order of v^2/f^2 . In the following, we denote the mass eigenstates of the SM gauge fields by W_L^\pm, Z_L, A_L and the new heavy gauge bosons by W_H^\pm, Z_H, B_H . The masses of the neutral gauge bosons are given to $O(v^2/f^2)$ ^[12, 16]

$$\begin{aligned} M_{A_L}^2 &= 0, \\ M_{B_H}^2 &= (M_Z^{\text{SM}})^2 s_W^2 \left\{ \frac{f^2}{5s'^2 c'^2 v^2} - 1 + \frac{v^2}{2f^2} \left[\frac{5(c'^2 - s'^2)^2}{2s_W^2} - \chi_H \frac{g}{g'} \frac{c'^2 s^2 + c^2 s'^2}{cc' ss'} \right] \right\}, \\ M_{Z_L}^2 &= (M_Z^{\text{SM}})^2 \left\{ 1 - \frac{v^2}{f^2} \left[\frac{1}{6} + \frac{1}{4}(c^2 - s^2)^2 + \frac{5}{4}(c'^2 - s'^2)^2 \right] + 8 \frac{v'^2}{v^2} \right\}, \\ M_{Z_H}^2 &= (M_W^{\text{SM}})^2 \left\{ \frac{f^2}{s^2 c^2 v^2} - 1 + \frac{v^2}{2f^2} \left[\frac{(c^2 - s^2)^2}{2c_W^2} + \chi_H \frac{g'}{g} \frac{c'^2 s^2 + c^2 s'^2}{cc' ss'} \right] \right\}, \end{aligned} \quad (10)$$

Where $\chi_H = \frac{5}{2} g g' \frac{scs'c'(c^2 s'^2 + s^2 c'^2)}{5g^2 s'^2 c'^2 - g'^2 s^2 c^2}$, $v=246$ GeV is the electroweak scale, v' is the vev of the scalar $SU(2)_L$ triplet, $s_W(c_W)$ represents the sine (cosine) of the weak mixing angle.

The phenomenologies of the littlest Higgs model at high energy colliders depend on the following parameters:

$$f, \quad c, \quad c', \quad x_\lambda.$$

$x_\lambda = \lambda_1/\lambda_2$, and one of λ_1, λ_2 can be replaced by the top-quark mass. Global fits to the experimental data put rather severe constraints on the $f > 4$ TeV at 95% C.L.^[17]. However, their analyses are based on a simple assumption that the SM fermions are charged only under $U(1)_1$. If the SM fermions are charged under $U(1)_1 \times U(1)_2$, the bounds become relaxed. The scale parameter $f = 1\text{--}2$ TeV is allowed for the mixing parameters c and c' in the ranges of 0–0.5 and 0.62–0.73, respectively^[18].

3 The cross sections of the processes $e^- \gamma \rightarrow e^- \gamma B_H, e^- Z B_H$

Taking account of the gauge invariance of the Yukawa couplings, one can write the couplings of the neutral gauge bosons γ, Z and B_H to the electron pair in the form of $i\gamma^\mu (g_V + g_A \gamma^5)$ with^[12, 19]

$$\begin{aligned} g_V^{\gamma ee} &= -e, & g_A^{\gamma ee} &= 0, \\ g_V^{Z ee} &= -\frac{g}{2c_W} \left\{ \left(-\frac{1}{2} + 2s_W^2 \right) - \frac{v^2}{f^2} \left[-c_W \chi_Z^{W'} c / 2s + \frac{s_W \chi_Z^{B'}}{s' c'} \left(2y_e - \frac{9}{5} + \frac{3}{2} c'^2 \right) \right] \right\}, \\ g_A^{Z ee} &= -\frac{g}{2c_W} \left\{ \frac{1}{2} - \frac{v^2}{f^2} \left[c_W \chi_Z^{W'} c / 2s + \frac{s_W \chi_Z^{B'}}{s' c'} \left(-\frac{1}{5} + \frac{1}{2} c'^2 \right) \right] \right\}, \\ g_V^{B_H ee} &= \frac{g'}{2s' c'} \left(2y_e - \frac{9}{5} + \frac{3}{2} c'^2 \right), \\ g_A^{B_H ee} &= \frac{g'}{2s' c'} \left(-\frac{1}{5} + \frac{1}{2} c'^2 \right). \end{aligned} \quad (11)$$

Here, $\chi_Z^{B'} = \frac{5}{2s_W} s' c' (c'^2 - s'^2)$ and $\chi_Z^{W'} = \frac{1}{2c_W} s c (c^2 - s^2)$. The $U(1)$ hypercharge of electron, y_e , can be fixed by requiring that the $U(1)$ hypercharge assignment is anomaly free, i.e., $y_e = \frac{3}{5}$. This is only one example among several alternatives for the $U(1)$ hypercharge choice^[12].

With the above couplings, B_H can be produced associated with a γ or Z boson via $e^- \gamma$ collision. At the tree-level, the relevant Feynman diagrams for the processes $e^- \gamma \rightarrow e^- \gamma B_H, e^- Z B_H$ in the littlest Higgs model are shown in Figs. 1(a)–(f).

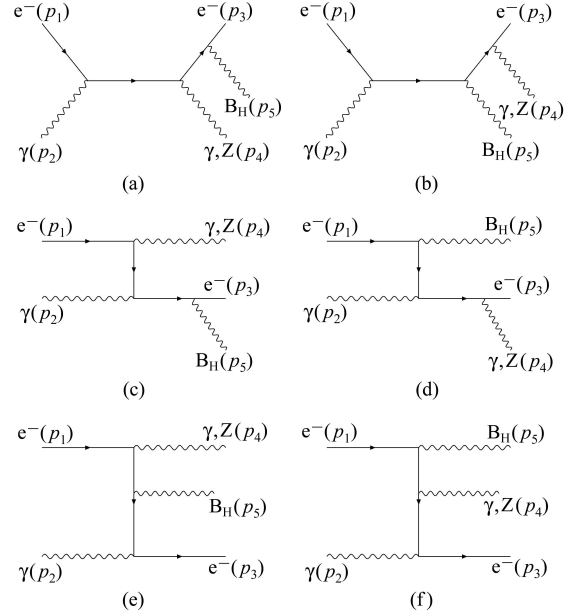


Fig. 1. The Feynman diagrams of the processes $e^- \gamma \rightarrow e^- \gamma B_H, e^- Z B_H$ in the littlest Higgs model.

In our calculations, we neglect the electron mass and define some notations as follows

$$\begin{aligned} G(p) &= \frac{1}{p^2}, \\ \Lambda^{V_i ee} &= g_V^{V_i ee} + g_A^{V_i ee} \gamma^5, \\ \Lambda^{B_H ee} &= g_V^{B_H ee} + g_A^{B_H ee} \gamma^5, \end{aligned} \quad (12)$$

where V_i presents the SM gauge boson γ or Z , and $G(p)$ denotes the propagator of the electron. The production amplitudes of the processes can be written as

$$M_{V_i} = M_{V_i}^a + M_{V_i}^b + M_{V_i}^c + M_{V_i}^d + M_{V_i}^e + M_{V_i}^f, \quad (13)$$

with

$$\begin{aligned} M_{V_i}^a &= G(p_1 + p_2) G(p_3 + p_5) \bar{u}_e(p_3) \not{\epsilon}(p_5) \Lambda^{B_H ee}(\not{p}_3 + \not{p}_5) \not{\epsilon}(p_4) \Lambda^{V_i ee}(\not{p}_1 + \not{p}_2) \not{\epsilon}(p_2) \Lambda^{\gamma ee} u_e(p_1), \\ M_{V_i}^b &= G(p_1 + p_2) G(p_3 + p_4) \bar{u}_e(p_3) \not{\epsilon}(p_4) \Lambda^{V_i ee}(\not{p}_3 + \not{p}_4) \not{\epsilon}(p_5) \Lambda^{B_H ee}(\not{p}_1 + \not{p}_2) \not{\epsilon}(p_2) \Lambda^{\gamma ee} u_e(p_1), \\ M_{V_i}^c &= G(p_1 - p_4) G(p_3 + p_5) \bar{u}_e(p_3) \not{\epsilon}(p_5) \Lambda^{B_H ee}(\not{p}_3 + \not{p}_5) \not{\epsilon}(p_2) \Lambda^{\gamma ee}(\not{p}_1 - \not{p}_4) \not{\epsilon}(p_4) \Lambda^{V_i ee} u_e(p_1), \\ M_{V_i}^d &= G(p_1 - p_5) G(p_3 + p_4) \bar{u}_e(p_3) \not{\epsilon}(p_4) \Lambda^{V_i ee}(\not{p}_3 + \not{p}_4) \not{\epsilon}(p_2) \Lambda^{\gamma ee}(\not{p}_1 - \not{p}_5) \not{\epsilon}(p_5) \Lambda^{B_H ee} u_e(p_1), \\ M_{V_i}^e &= G(p_3 - p_2) G(p_1 - p_4) \bar{u}_e(p_3) \not{\epsilon}(p_2) \Lambda^{\gamma ee}(\not{p}_3 - \not{p}_2) \not{\epsilon}(p_5) \Lambda^{B_H ee}(\not{p}_1 - \not{p}_4) \not{\epsilon}(p_4) \Lambda^{V_i ee} u_e(p_1), \\ M_{V_i}^f &= G(p_3 - p_2) G(p_1 - p_5) \bar{u}_e(p_3) \not{\epsilon}(p_2) \Lambda^{\gamma ee}(\not{p}_3 - \not{p}_2) \not{\epsilon}(p_4) \Lambda^{V_i ee}(\not{p}_1 - \not{p}_5) \not{\epsilon}(p_5) \Lambda^{B_H ee} u_e(p_1). \end{aligned} \quad (14)$$

The hard photon beams of the $e\gamma$ collision can be obtained from laser backscattering at the e^+e^- linear collider. Here we denote \hat{s} and s as the c.m. energies of the $e\gamma$ and e^+e^- systems, respectively. Using the above amplitudes, we can directly obtain the cross sections $\hat{\sigma}(\hat{s})$ of the sub-processes $e^- \gamma \rightarrow e^- \gamma B_H$, $e^- Z B_H$, and the total cross sections at the e^+e^- linear collider can be obtained by folding $\hat{\sigma}(\hat{s})$ with the photon distribution function $f_\gamma(x)$ which is given in Ref. [20],

$$\sigma_{\text{tot}}(s) = \int_{M_{\text{final}}^2/s}^{x_{\text{max}}} dx \hat{\sigma}(\hat{s}) f_\gamma(x). \quad (15)$$

M_{final} is the sum of the masses of the final state particles and

$$f_\gamma(x) = \frac{1}{D(\xi)} \left[1 - x + \frac{1}{1-x} - \frac{4x}{\xi(1-x)} + \frac{4x^2}{\xi^2(1-x)^2} \right], \quad (16)$$

with

$$D(\xi) = \left(1 - \frac{4}{\xi} - \frac{8}{\xi^2} \right) \ln(1+\xi) + \frac{1}{2} + \frac{8}{\xi} - \frac{1}{2(1+\xi)^2}. \quad (17)$$

In the above equations, $\xi = 4E_e\omega_0/m_e^2$ in which m_e and E_e stand, respectively, for the incident electron mass and energy. ω_0 stands for the laser photon energy, and $x = \omega/E_e$ stands for the fraction of energy of the incident electron carried by the back-scattered photon. f_γ vanishes for $x > x_{\text{max}} = \omega_{\text{max}}/E_e = \xi/(1+\xi)$. In order to avoid the creation of e^+e^- pairs by the interaction of the incident and back-scattered photons, we require $\omega_0 x_{\text{max}} \leq m_e^2/E_e$ which implies $\xi \leq 2+2\sqrt{2} \approx 4.8$. For the choice of $\xi = 4.8$, we obtain

$$x_{\text{max}} \approx 0.83, \quad D(\xi) \approx 1.8.$$

For simplicity, we have ignored the possible polarization for the electron and photon beams.

Because we have neglected the electron mass in our calculations, the processes have t-channel collinear and soft IR divergences for outgoing photon. On the other hand, we should take account of the capability of experimental detections. So we take the cuts on rapidity y and the transverse momenta p_T of all the final states as they are usually taken

$$|y| < 1.5, \quad p_T > 20 \text{ GeV}. \quad (18)$$

4 The numerical results and conclusions

To obtain numerical results, we take $M_Z = 91.187 \text{ GeV}$, $v = 246 \text{ GeV}$, $s_W^2 = 0.23$. The electromagnetic fine structure constant α_e at certain energy scale is calculated from the simple QED one-loop evolution formula with the boundary value $\alpha_e =$

$1/137.04^{[21]}$. There are four free parameters in our numerical estimations, i.e., f, c, c', \sqrt{s} . Here, we take the parameter spaces ($f=1-2 \text{ TeV}$, $c=0-0.5$, $c'=0.62-0.73$) which are consistent with the electroweak precision data. The final numerical results are summarized in Figs. 2—3.

From Eqs. (10) and (11), we can see that the mixing parameter c can affect the B_H mass and the coupling $Z\bar{e}e$ which are related to the cross sections, but c only exists in the modified terms of order v^2/f^2 . Therefore, the production cross sections of the processes $e^- \gamma \rightarrow e^- \gamma B_H$, $e^- Z B_H$ are not sensitive to c , and we fix the value of c as 0.4 in our calculations. The cross sections mainly depend on the mixing parameter c' . In Fig. 2, we plot the cross sections as a function of the parameter c' , taking $\sqrt{s} = 0.8 \text{ TeV}$ and $f=1 \text{ TeV}$, 2 TeV as the examples. From Fig. 2, one can see that the cross sections drop sharply to zero when c' equals $\sqrt{2/5}$. This is because the coupling of the gauge boson B_H to the electron pair becomes decoupled with $c' = \sqrt{2/5}$. When c' is over $\sqrt{2/5}$, the cross sections increase with c' and the cross section of the process $e^- \gamma \rightarrow e^- \gamma B_H$ can reach the level of a few fb in some parameter spaces. But the cross section of the process $e^- \gamma \rightarrow e^- Z B_H$ is much smaller than that of $e^- \gamma \rightarrow e^- \gamma B_H$ and its maximum can only reach the level of 10^{-1} fb . So the process $e^- \gamma \rightarrow e^- \gamma B_H$ should have advantage in probing B_H . On the other hand, comparing the results for $f=1 \text{ TeV}$ with those for $f=2 \text{ TeV}$, we find that the cross sections decrease slightly with f increasing. This is mainly because the mass of B_H increases with f increasing which can depress the phase space.

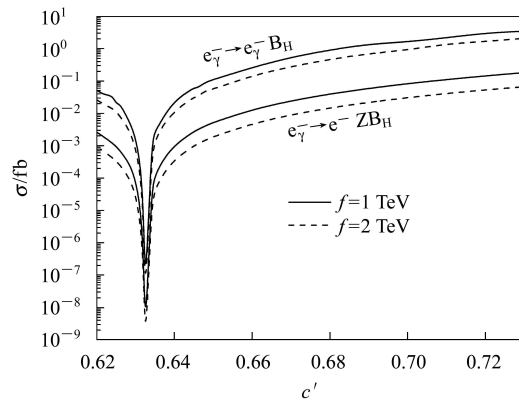


Fig. 2. The production cross sections of the processes $e^- \gamma \rightarrow e^- \gamma B_H$ (upper curves) and $e^- \gamma \rightarrow e^- Z B_H$ (lower curves) as a function of the mixing parameter c' for $\sqrt{s} = 800 \text{ GeV}$ and the scale parameter $f = 1 \text{ TeV}$ (solid line), and $f = 2 \text{ TeV}$ (dashed line), respectively.

To show the influence of the c.m. energy \sqrt{s} on the cross sections, we plot the cross sections as a function of \sqrt{s} with $f=1 \text{ TeV}$ and $c' = 0.65, 0.70$ in Fig.3.

Taking account of the c.m. energy at the ILC and the kinetic limit, we present the numerical results for energies ranging from 0.5 to 1.5 TeV. The results show that the cross section of $e^- \gamma B_H$ production slightly decreases with \sqrt{s} increment and the cross section of $e^- Z B_H$ production is more insensitive to \sqrt{s} .

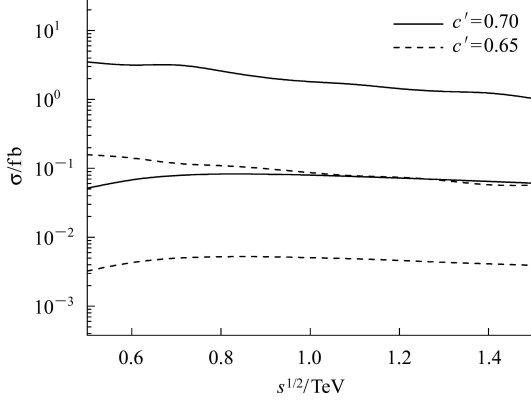


Fig. 3. The production cross sections of the processes $e^- \gamma \rightarrow e^- \gamma B_H$ (upper solid and dashed lines) and $e^- \gamma \rightarrow e^- Z B_H$ (lower solid and dashed lines) as a function of the c.m. energy \sqrt{s} for $f = 1$ TeV and the mixing parameter $c' = 0.70$ (solid line), and $c' = 0.65$ (dashed line), respectively.

The yearly luminosity of the ILC can reach 500 fb^{-1} . So we can conclude that hundreds typical B_H events can be produced via the process $e^- \gamma \rightarrow e^- \gamma B_H$ in the sizable parameter spaces each year, but the cross section of the process $e^- \gamma \rightarrow e^- Z B_H$ is too small to produce enough signals. The process $e^- \gamma \rightarrow e^- \gamma B_H$ should be more promising to probe B_H . But to detect B_H , one also needs to study the decay modes of B_H and such study has been done in Ref. [12]. The decay width of a particle affects how and to what extent it is experimentally detectable, since the production of particles with very large decay widths may be difficult to be distinguished from background processes. For B_H , the parameter spaces where the large decay width would occur are beyond current search limits in any case. So if B_H would be produced it can be detected via the measurement of the peak in the invariant mass distribution of its decaying particles. On the other hand, for the process $e^- \gamma \rightarrow e^- \gamma B_H$, the backgrounds are likely to be much large in the collision direction because it is difficult to distinguish the final state $e^- \gamma$ from the injecting $e^- \gamma$. So the backgrounds can be significantly depressed when we take the cuts on the final states, which has been done in our calculation.

In the following, we focus on discussing how to detect B_H via its decay modes. The main decay modes of B_H are $e^+ e^- + \mu^+ \mu^- + \tau^+ \tau^-$, $d\bar{d} + s\bar{s}$, $u\bar{u} + c\bar{c}$, ZH ,

$W^+ W^-$. The decay branching ratios of these modes have been studied in Ref. [12] which are strongly dependent on the $U(1)$ charge assignments of the SM fermions. In general, the heavy gauge bosons are likely to be discovered via their leptonic decay modes. For B_H , the most interesting decay modes should be $e^+ e^-$, $\mu^+ \mu^-$. This is because such leptons can be easily identified and the number of $e^+ e^-$, $\mu^+ \mu^-$ background events with such a high invariant mass is very small. So, the measurement of the peaks in the invariant mass distributions of $e^+ e^-$, $\mu^+ \mu^-$ can provide a unique way to probe B_H . For the signal $e^- \gamma e^+ e^- (\mu^+ \mu^-)$, the main SM background arises from $e^- \gamma \rightarrow e^- \gamma Z$ with $Z \rightarrow e^+ e^- (\mu^+ \mu^-)$. The cross section of such background is a few pb with $\sqrt{s} = 0.5\text{--}1.5$ TeV^[22]. For the signal $e^- Z e^+ e^- (\mu^+ \mu^-)$, the most serious SM backgrounds come from the processes $e^- \gamma \rightarrow e^- Z Z$, $e^- \gamma \rightarrow e^- Z H$ and their cross sections can reach about 10 fb, a few fb, respectively, in the energy range $\sqrt{s} = 0.5\text{--}1.5$ TeV^[23]. But one can very easily distinguish B_H from Z via their significantly different $e^+ e^- (\mu^+ \mu^-)$ invariant mass distributions. The background $e^- \gamma \rightarrow e^- Z H$ with H decaying to lepton pair or light quark pair is very small because the decay branching ratios of these H decay modes are strongly depressed by the small masses of leptons and light quarks. On the other hand, we can also distinguish B_H from H via their different invariant mass distributions of final particles because B_H is much heavier than H . As we know, in a narrow region around $c' = 0.63$, the decay branching ratios of $B_H \rightarrow l^+ l^-$ approach zero due to the decoupling of B_H with lepton pair. In this case, the main decay modes of B_H are $B_H \rightarrow W^+ W^-$, ZH . The decay mode $Z \rightarrow W^+ W^-$ is of course kinematically forbidden in the SM but $H \rightarrow W^+ W^-$ is the dominant decay mode with Higgs mass above 135 GeV (one or both of W is off-shell for Higgs mass below $2M_W$). So the background for the signal $e^- Z W^+ W^-$ might be serious and it is hard to detect the B_H via $e^- \gamma \rightarrow e^- Z B_H$ with $B_H \rightarrow W^+ W^-$. However, the process $e^- \gamma \rightarrow e^- \gamma B_H$ does not suffer such large background problem which would be another advantage of $e^- \gamma \rightarrow e^- \gamma B_H$. For $B_H \rightarrow ZH$, the main final states are $l^+ l^- b\bar{b}$. In this case, two b -jets can be reconstructed to the Higgs mass and a $l^+ l^-$ can be reconstructed to the Z mass. So the background is very clean. Furthermore, the decay mode ZH involves the off-diagonal coupling HZB_H and the factor $\cot 2\psi'$ in the coupling HZB_H is a unique feature of the littlest Higgs model. It should also be mentioned that experimental precise measurement of such off-diagonal coupling is much easier than that of diagonal coupling. So, the decay mode ZH would not only provide a better way to probe B_H but also provide a robust test of the littlest Higgs model.

As we have mentioned in the introduction, in the littlest Higgs model, another important B_H production process $e^- \gamma \rightarrow e^- B_H$ has been studied in Ref. [11]. In wide range of the parameter spaces preferred by the electroweak precision data, the cross section of $e^- \gamma \rightarrow e^- B_H$ is in the range from tens fb to hundreds fb, and B_H may be observed via its leptonic decay modes. The cross section of such process is much larger than those of $e^- \gamma \rightarrow e^- \gamma B_H$, $e^- Z B_H$. For the process $e^- \gamma \rightarrow e^- B_H$, the outgoing B_H and e^- concentrate in the direction of incoming $e^- \gamma$ beams due to the t-channel resonance effect. In this case, it is difficult to distinguish the outgoing e^- beams from the incoming e^- beams which may significantly enhance the backgrounds. But for the processes $e^- \gamma \rightarrow e^- \gamma B_H$, $e^- Z B_H$, the outgoing e^- beams are not so concentrated in the direction of the incoming $e^- \gamma$ beams. Detecting B_H together with the other final states may greatly depress the backgrounds. So our study can complement the probe of the new gauge

boson B_H via $e \gamma$ collision.

In conclusion, the realization of $e \gamma$ and $\gamma \gamma$ collisions at the planned ILC with high energy and luminosity will provide more chances to probe the new particles predicted by the new physics beyond the SM. In this paper, we study the new gauge boson B_H production processes via $e \gamma$ collision, i.e., $e^- \gamma \rightarrow e^- \gamma B_H$, $e^- Z B_H$. The study shows that the cross section of $e^- \gamma \rightarrow e^- Z B_H$ is less than 10^{-1} fb in most parameter spaces allowed by the electroweak precision data, and the cross section of the process $e^- \gamma \rightarrow e^- \gamma B_H$ can be over one fb for the favorable parameter spaces. We can predict that there are enough B_H signals produced via $e^- \gamma \rightarrow e^- \gamma B_H$ at the planned ILC. Because the new gauge boson B_H can be easily distinguished from the SM Z, H bosons, the signal would be typical and the backgrounds would be very clean. So, our study can complement the probe for B_H via $e^- \gamma$ collision.

References

- 1 Schmaltz M, Tucker-Smith D. *Ann. Rev. Nucl. Part. Sci.*, 2005, **55**: 229; HAN T, Logen H E, McElrath B et al. *JHEP*, 2006, **0601**: 099
- 2 Arkani-Hamed N, Cohen A G, Gregoire T et al. *JHEP*, 2002, **0208**: 020; Arkani-Hamed N, Cohen A G, Katz E et al. *JHEP*, 2002, **0208**: 021
- 3 Low I, Skiba W, Smith D. *Phys. Rev. D*, 2002, **66**: 072001; Skiba W, Terning J. *Phys. Rev. D*, 2003, **68**: 075001; Kaplan D E, Schmaltz M. *JHEP*, 2003, **0310**: 039
- 4 CHANG S, Wacker J G. *Phys. Rev. D*, 2004, **69**: 035002; CHANG S. *JHEP*, 2003, **0312**: 057
- 5 Arkani-Hamed N, Cohen A G, Katz E et al. *JHEP*, 2002, **0207**: 034
- 6 Perelstein M. *Prog. Part. Nucl. Phys.*, 2007, **58**: 247
- 7 Badelek B et al. *Inter. Jour. Mod. Phys. A*, 2004, **30**: 5097
- 8 Thlnov V I. *Acta Phys. Polon. B*, 2006, **37**: 1049; Telnov V I. *Acta Phys. Polon. B*, 2006, **37**: 633; Battaglia M, Barklow T, Peskin M E et al. hep-ex/0603010
- 9 Boos E et al. *Nucl. Instrum. Methods Phys. Res., Sect. A*, 2001, **472**: 100; Brodsky S J. *Int. J. Mod. Phys. A*, 2003, **18**: 2871
- 10 WANG X L, CHEN J H, LIU Y B et al. *Phys. Rev. D*, 2006, **74**: 015006
- 11 YUE C X, WANG W. *Phys. Rev. D*, 2005, **71**: 015002
- 12 HAN T, Logan H E, McElrath B et al. *Phys. Rev. D*, 2003, **67**: 095004
- 13 Logan H E. *Phys. Rev. D*, 2004, **70**: 115003
- 14 Buras A J, Poschenrieder A, Uhlig S. *Nucl. Phys. B*, 2005, **716**: 173; Choudhury S R, Gaur N, Joshi G C et al. hep-ph/0408125; Choudhury S R, Gaur N, Goyal A et al. *Phys. Lett. B*, 2004, **601**: 164
- 15 Park S C, SONG J. *Phys. Rev. D*, 2004, **69**: 115010; Hubisz J, Meade P. *Phys. Rev. D*, 2005, **71**: 035016; Schmaltz M, Tucker-Smith D. *Ann. Rev. Nucl. Part. Sci.*, 2005, **55**: 229; Kilian W, Reuter J. *Phys. Rev. D*, 2004, **70**: 015004; Blanke M, Buras A J et al. *JHEP*, 2007, **0701**: 066; CHEN M C, Dawson S. *Phys. Rev. D*, 2004, **70**: 015003; CHEN M C. *Mod. Phys. Lett. A*, 2006, **21**: 621; Casalbuoni R, Deandrea A, Oertel M. *JHEP*, 2004, **0402**: 032
- 16 Conley J A, Hewett J, Le M P. *Phys. Rev. D*, 2005, **72**: 115014
- 17 Hewett J L, Petriello F J et al. *JHEP*, 2003, **0310**: 062; Csaki C, Hubisz J, Kribs G D et al. *Phys. Rev. D*, 2003, **67**: 115002
- 18 Csaki C, Hubisz J, Kribs G D et al. *Phys. Rev. D*, 2003, **68**: 035009; Gregoire T, Smith D R, Wacker J G. *Phys. Rev. D*, 2004, **69**: 115008
- 19 Buras A J, Poschenrieder A et al. *JHEP*, 2006, **0611**: 062
- 20 Jikia G. *Nucl. Phys. B*, 1992, **374**: 83; Eboli O J P et al. *Phys. Rev. D*, 1993, **47**: 1889; Cheung K M. *ibid.*, 1993, **47**: 3750
- 21 Donoghue J F, Golowich E, Holstein B R. *Dynamics of the Standard Model*. Cambridge: Cambridge University Press, 1992. 34
- 22 Dittmaier S, Böhm M. *Nucl. Phys. B*, 1994, **412**: 39
- 23 Eboli O J P, González-García M C, Novaes S F. *Nucl. Phys. B*, 1994, **411**: 381; Cheung K. *Nucl. Phys. B*, 1993, **403**: 572